ACS Catalysis

Research Article

pubs.acs.org/acscatalysis

Investigation into the Equilibrium of Iridium Catalysts for the Hydroformylation of Olefins by Combining In Situ High-Pressure FTIR and NMR Spectroscopy

Christoph Kubis,*[,†] Wolfgang Baumann,[†] Enrico Barsch,[†,‡] Detlef Selent,[†] Mathias Sawall,[§] Ralf Ludwig,[†,‡] Klaus Neymeyr,[†,§] Dieter Hess,[⊥] Robert Franke,[⊥,∥] and Armin Börner*[,†,‡]

[†]Leibniz-Institut für Katalyse e.V. an der Universität Rostock, Albert-Einstein Str. 29a, D-18059 Rostock, Germany

[‡]Institut für Chemie, Universität Rostock, Albert-Einstein Str. 3, D-18059 Rostock, Germany

[§]Institut für Mathematik, Universität Rostock, Ulmenstrasse 69, D-18057 Rostock, Germany

[⊥]Evonik Industries AG, Paul-Baumann-Str. 1, D-45772 Marl, Germany

[∥]Lehrstuhl für Theoretische Chemie, Ruhr-Universität Bochum, D-44780 Bochum, Germany

Supporting Information

ABSTRACT: A detailed quantitative study of phosphine-modified hydrido iridium complexes relevant for the hydroformylation reaction has been performed using HP-FTIR and HP-NMR spectroscopy. The equilibrium composition under typical reaction conditions has been characterized. Investigation of the temperature dependency allowed even for a distinction between both configurational isomers of $[HIr(CO)_2(PPh_3)_2]$. The trihydride complex $[H_3Ir(CO)(PPh_3)_2]$ is part of the investigated equilibrium depending on the ratio of $p(H_2)/p(CO)$. Single rate constants for the sequence of corresponding equilibrium reactions have been estimated from stopped-flow experiments and conventional measurements, monitoring the concentrations after changing reactant concentrations.

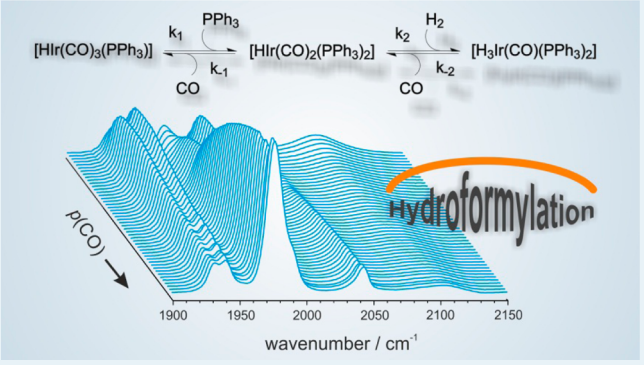

KEYWORDS: *homogeneous catalysis, hydroformylation, iridium, FTIR spectroscopy, NMR spectroscopy, DFT calculations*

INTRODUCTION

The homogeneously catalyzed hydroformylation of alkenes using catalysts based on rhodium and cobalt is of significant industrial importance.[1−4] Large-scale processes for different feedstocks have been established for producing a range of aldehydes and alcohols, which are utilized as intermediates or final products in plasticizers, detergents, surfactants, pharmaceutical products, aroma compounds, and as solvents. The economic relevance of the hydroformylation reaction induced great efforts in industrial and academic research in the fields of novel catalysts for improvement of the catalytic performance as well as kinetic and mechanistic understanding.

There is currently much interest in catalytic systems based on transition metals other than cobalt and rhodium.[5−14] Different reasons are discussed in the literature. The price of rhodium metal from which very active and chemo-/regioselective catalysts can be formed is high and most notably volatile, because it is strongly correlated with changes in the automotive industry (~80% of the world Rh production is used for catalytic converters in automobiles). Catalysts derived from cobalt are less costly, but Co-based processes are run at more severe reaction conditions, which lead to higher investment costs. The higher reducing activity of cobalt catalysts can be advantageous for the production of alcohols but especially with phosphine-modified catalysts, hydrogenation toward the alkanes is a considerable issue.[2b] A number of other transition metals (e.g., Ru, Ir, Pd, Pt, Fe) are generally capable of forming complexes active as hydroformylation catalysts.[5] However, over the years, most research activities were focused on catalysts based on rhodium and cobalt. Significantly less information is available about the hydroformylation with other transition metal catalysts.

Kinetic and mechanistic studies are important from academic and industrial viewpoints. The technical basis for these are provided by in situ spectroscopic measurements at actual reaction conditions.[15,16] For the hydroformylation reaction, which is performed at high pressures and temperatures, sophisticated devices for FTIR and NMR spectroscopy have been constructed. Both spectroscopic methods in combination deliver currently the most comprehensive information about

Received: March 20, 2014
Revised: May 11, 2014
Published: May 12, 2014

   dx.doi.org/10.1021/cs500368z | ACS Catal. 2014, 4, 2097−2108

the catalytic cycle. In addition, labeling experiments and chromatographic analysis contribute substantially within the framework of such kinetic and mechanistic studies.

More often, in situ spectroscopic measurements (especially FTIR measurements) are accompanied by a chemometric treatment (factor analysis) of the data, which is necessary to get the maximum information from the experiments.[17,18] In principle, such a factor analysis can provide pure component spectra and their associated concentration profiles. In unmodified hydroformylation and other homogeneous catalytic reactions, the algorithm BTEM (band target entropy minimization) developed by Garland has been extensively applied.[19−24] With this tool they are able to identify carbonyl species present in the ppm to subppm concentration range. A typical example is the long-sought [$HRh(CO)_4$] in the unmodified rhodium-catalyzed hydroformylation.[25] The application of BTEM by Garland's group in fundamental studies of the bimetallic catalytic binuclear elimination reaction (CBER) played a decisive role for the spectroscopic identification and quantification of respective key intermediates relevant for the analysis of the mechanisms.[26−32] Another algorithm for factor analysis is the PCD code (pure component decomposition) developed by Neymeyr and Sawall. It has been applied to ligand-modified hydroformylations, equilibrium reactions of rhodium complexes, and photocatalytic water splitting.[33−38]

In order to assign experimental infrared spectra to molecular structures, the calculation of vibrational spectra via DFT methods is of crucial value. This is especially important for new and not isolatable intermediates.[20,35,38−44]

IRIDIUM-CATALYZED HYDROFORMYLATION

Recently, it has been found that iridium complexes with triphenylphosphine as a ligand catalyze the hydroformylation of 1-alkenes to give aldehydes with considerable activities. A comparison of the TOF values with a relevant rhodium system showed that the iridium system is about 8 times slower.[9,44] Hess et al. found in an in situ spectroscopic study that during the hydroformylation reaction the catalytic species consist of a mixture of hydrido complexes.[44] They could interpret the infrared spectra, which were extracted from spectral series via chemometric methods with the help of DFT calculations. In their study, a quantification of the different iridium complexes could not be realized.

A detailed structural and quantitative description of the catalyst system, which often represents a mixture of several components, is the basis of any kinetic and mechanistic study. It has to be noted that due to the higher stability of iridium carbonyl complexes compared to rhodium congeners they have been frequently used as model complexes in mechanistic studies.[45−54] Many complex structures have been thoroughly characterized, but mostly no quantitative informations are available when dealing with mixtures of complexes.

The study presented herein will contain a quantitative analysis of iridium carbonyl hydrides at practically relevant reaction conditions and carves out some interesting and new aspects with respect to iridium carbonyl complexes and their spectroscopic characterization.

RESULTS AND DISCUSSION

Characterization of Hydrido Complexes in *n*-Hexane. In order to have a detailed knowledge of the catalytically relevant species under reaction conditions, we performed a series of in situ FTIR experiments related to studies of Beller and Hess.[9,44] We conducted our initial FTIR experiments in *n*-hexane as solvent in order to have a reliable comparison with data from the literature.[55−63] For the NMR measurements, toluene has been used as a solvent. A first trial was initiated by mixing [(acac)Ir(COD)] ([Ir] = 0.9 mM) with 4 equivalents of triphenylphosphine at 100 °C, $p(CO)$ = 1 MPa and $p(H_2)$ = 1 MPa. In accordance with other investigations, we also found that after the preformation period, one gets a mixture of hydrido complexes.

Assignments of the spectral contributions to complex structures have been performed with the help of DFT-calculated vibrational spectra, deuteration experiments, and NMR spectroscopy. A full set of experimental and DFT-calculated infrared spectra of hydrido and deuterido complexes as well as related NMR spectroscopic data can be found in the Supporting Information. Our results are in good agreement with data in the literature.[55−64] Figure 1 shows the experimental

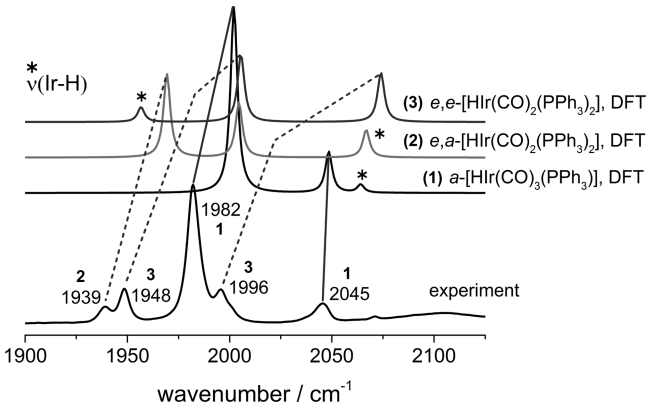

Figure 1. Experimentally obtained infrared spectrum of a mixture of iridium hydrido complexes and calculated spectra via DFT methods for different molecular structures. Reaction conditions for the experiment: [Ir] = 0.9 mM, [PPh_3] = 3.6 mM, θ = 100 °C, $p(CO)$ = 1 MPa, $p(H_2)$ = 1 MPa, solvent = *n*-hexane.

spectrum of the hydrido complex mixture as well as the calculated spectra via DFT methods for comparison. Whereas the assignment of the carbonyl vibrational bands $\nu(CO)$ = 1982 and 2045 cm^{-1} to *a*-[$HIr(CO)_3(PPh_3)$] is directly possible on the basis of DFT-calculated spectra, the analysis of both stereoisomers *e,e*-[$HIr(CO)_2(PPh_3)_2$] ($\nu(CO)$ = 1948, 1996 cm^{-1}) and *e,a*-[$HIr(CO)_2(PPh_3)_2$] ($\nu(CO)$ = 1939, 1985 (obscured) cm^{-1}) is not straightforward. It was found that those contributions resulting from hydride vibrations which are not coupled with a carbonyl vibration (missing H-M-CO-*trans* relation) give bands in the calculated spectra (please note the markings for ν(Ir−H) in Figure 1), but they are not detected in the experimental spectrum under the applied conditions. Deuteration experiments performed in this study confirmed the aforementioned assignment.[61,55,58] In the case of a H-M-CO-*trans* relation, such coupled vibrational contributions are shifted in the spectrum as a result of the hydride/deuteride exchange.

Scheme 1 gives an overview of spectroscopic data for relevant hydrido and deuterido complexes. As a result of our deuteration experiments and DFT calculations, other stereoisomeric structures can be excluded.

Hydroformylation Reaction of 3,3-Dimethyl-1-butene in Toluene. In order to investigate the composition of iridium

dx.doi.org/10.1021/cs500368z | ACS Catal. 2014, 4, 2097−2108

Scheme 1. FTIR Spectroscopic Data for Hydrido and Deuterido Complexes Measured in *n*-Hexane at 30 °C (see Supporting Information for Further Experimental Details)

	a-[HIr(CO)$_3$(PPh$_3$)]	*e,e*-[HIr(CO)$_2$(PPh$_3$)$_2$]	*e,a*-[HIr(CO)$_3$(PPh$_3$)$_2$]
hydrido complex	ν(CO) = 1982, 2045 cm^{-1}	ν(CO) = 1948, 1996 cm^{-1}	ν(CO) = 1938, 1985 cm^{-1}
deuterido complex	ν(CO) = 1982, 2045 cm^{-1}	ν(CO) = 1957, 2017 cm^{-1}	ν(CO) = 1938, 1985 cm^{-1}

complexes under hydroformylation conditions, an experiment with 3,3-dimethyl-1-butene was carried out in toluene. Prior to the addition of the olefin, the following catalyst preformation routine has been conducted: At 100 °C [(acac)Ir(COD)] and 4 equivalents triphenylphosphine were treated first with 0.9 MPa of carbon monoxide. Upon addition of CO, [(acac)Ir(CO)$_2$] (ν(CO) = 1996, 2071 cm^{-1}) and an uncharacterized complex (ν(CO) = 1962 cm^{-1}) were formed. Then 0.9 MPa of hydrogen was added starting the formation of hydrido complexes: *a*-[HIr(CO)$_3$(PPh$_3$)] (ν(CO) = 1977, 2043 cm^{-1}), *e,a*-[HIr(CO)$_2$(PPh$_3$)$_2$] (ν(CO) = 1931, 1980 (obsc.) cm^{-1}), and *e,e*-[HIr(CO)$_2$(PPh$_3$)$_2$] (ν(CO) = 1941, 1990 cm^{-1}). Figure 2 shows FTIR spectra collected during this

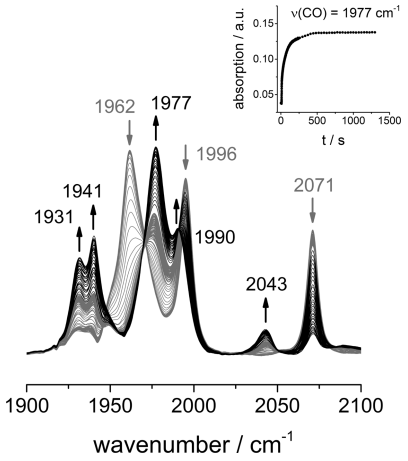

Figure 2. FTIR spectra collected during the formation of hydrido complexes: *a*-[HIr(CO)$_3$(PPh$_3$)] (ν(CO) = 1977, 2043 cm^{-1}), *e,a*-[HIr(CO)$_2$(PPh$_3$)$_2$] (ν(CO) = 1931, 1980 cm^{-1}) (band at 1980 cm^{-1} was obscured), and *e,e*-[HIr(CO)$_2$(PPh$_3$)$_2$] (ν(CO) = 1941, 1990 cm^{-1}) initiated by addition of 0.9 MPa of hydrogen from a mixture of [(acac)Ir(CO)$_2$] (ν(CO) = 1996, 2071 cm^{-1}) and a structurally uncharacterized complex (ν(CO) = 1962 cm^{-1}), which were generated after treatment with CO of a solution of [(acac)Ir(COD)] and PPh$_3$. Experimental conditions: [Ir] = 5.0 mM, [PPh$_3$] = 20 mM, θ = 100 °C, p(CO) = 0.9 MPa, p(H$_2$) = 0.9 MPa, solvent = toluene. Gray spectra: reaction start to 30.1 s in 0.288 s intervals; black spectra: 35.8 to 237.3 s in 5.76 s intervals.

reaction after different time intervals. The formation of hydrido complexes with reference to the band position ν(CO) = 1977 cm^{-1} for *a*-[HIr(CO)$_3$(PPh$_3$)] is completed within ca. 12 min.

3,3-Dimethyl-1-butene was selected as a substrate because of its incapability of double bond isomerization, which would alter the kinetics. This olefin is frequently used as a model substrate in kinetic and in situ spectroscopic studies.[24,34,35,65−67] The hydroformylation was started by the injection of the olefin via a syringe pump. The partial pressures were set to p(CO) = 1 MPa and p(H$_2$) = 1 MPa, kept constant by a constant pressure controller with synthesis gas (p(CO)/p(H$_2$) = 1) as the supplied gas. The reaction was monitored by in situ FTIR spectroscopy and parallel GC analysis for which liquid samples were taken by means of an automatic sampling device. For concentration data of the organic products, see Figure 3a.

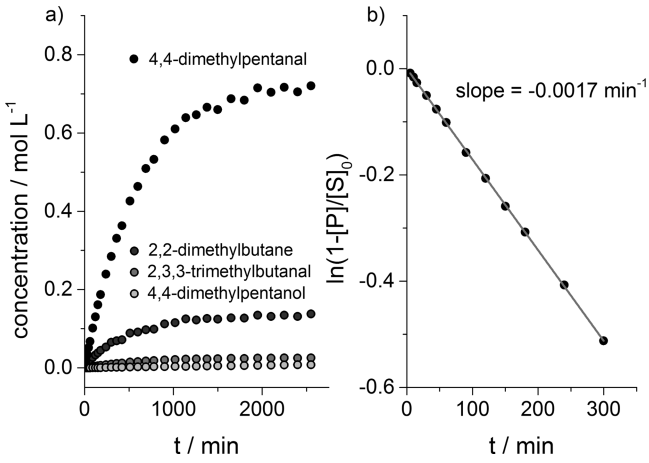

Figure 3. (a) Product concentration profiles for the hydroformylation of 3,3-dimethyl-1-butene based on GC analysis. Product selectivities: 4,4-dimethylpentanal = 81.1%, 2,3,3-trimethylbutanal = 2.8%, 4,4-dimethylpentanol = 0.6%, 2,2-dimethylbutane = 15.5%. (b) Determination of the pseudo-first-order rate constant of the overall reaction. Experimental conditions: [Ir] = 5.0 mM, [PPh$_3$] = 20 mM, [olefin] = 0.9 M, θ = 100 °C, p(CO) = 1 MPa, p(H$_2$) = 1 MPa, solvent = toluene.

The overall reaction can be considered formally as a pseudo-first-order parallel reaction with the products 4,4-dimethylpentanal, 2,3,3-trimethylbutanal, 2,2-dimethylbutane, and 4,4-dimethylpentanol formed with the same reaction order but different selectivities. Consequently, the selectivities are almost constant for the whole conversion range. From the sum of all product concentrations, a pseudo-first-order rate constant was calculated with k^{obs} = 0.0017 min^{-1} (Figure 3b). Because we used synthesis gas (p(CO)/p(H$_2$) = 1) as a supplying gas for the constant pressure controller unit, partial pressures are slightly changed due to formation of the alkane. Therefore, the determination of the rate constant was based on data up to 40% conversion.

We like to mention briefly that the high *n*-regioselectivity with 96.7% originates from the steric hindrance of the substrate 3,3-dimethyl-1-butene. This has been already discussed for modified and unmodified rhodium catalysts.[68] The high chemoselectivity for the alkane with 15.5% is a serious problem using nonpolar solvents. Better results can be obtained for reactions performed in polar solvents or by addition of

dx.doi.org/10.1021/cs500368z | ACS Catal. 2014, 4, 2097−2108

inorganic salts.[8,9] However, because our focus in this study is a quantitative description of the catalytically relevant iridium complexes by FTIR and NMR spectroscopy, we did depend on a suitable solvent for the experiments for which we selected toluene.

FTIR spectra were collected during the entire reaction (see Figure 4). From the reaction start until complete conversion, the composition of the hydrido complexes *a*-[$HIr(CO)_3(PPh_3)$] and *e,a/e,e*-[$HIr(CO)_2(PPh_3)_2$] did not change.

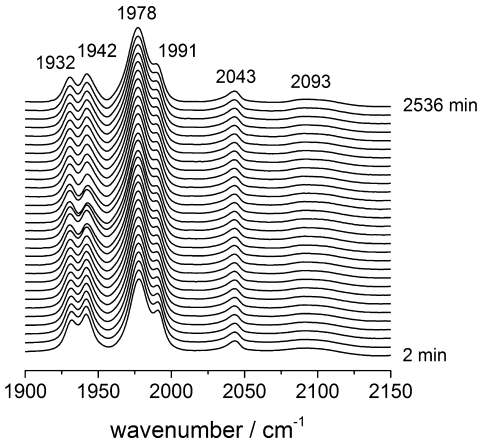

Figure 4. FTIR spectra registered during the hydroformylation of 3,3-dimethyl-1-butene. Experimental conditions: [Ir] = 5.0 mM, [PPh_3] = 20 mM, [olefin] = 0.9 M, θ = 100 °C, $p(CO)$ = 1 MPa, $p(H_2)$ = 1 MPa, solvent = toluene. Spectroscopic assignments: *a*-[$HIr(CO)_3(PPh_3)$] (ν(CO) = 1978, 2043 cm^{-1}), *e,a*-[$HIr(CO)_2(PPh_3)_2$] (ν(CO) = 1931, 1980 (obsc.) cm^{-1}), and *e,e*-[$HIr(CO)_2(PPh_3)_2$] (ν(CO) = 1941, 1991 cm^{-1}). The band at 2093 cm^{-1} has been assigned to [$HIr(CO)_2(PPh_3)_2$] without a relation to one specific stereoisomer. The background spectrum used was measured from a mixture of toluene and 3,3-dimethyl-1-butene under the same conditions.

No other intermediates such as frequently observed acyl complexes were found.[1,16,19] The overall pseudo-first-order kinetics and the absence of any substrate complexes are in line with each other and have been discussed in the literature to originate from a rate control by the early steps in the reaction cycle.[1,69]

Because there is a mixture of hydrido complexes relevant for the catalytic reaction we were furthermore interested in a quantification of the equilibrium composition.

Influence of CO Partial Pressure on the Equilibrium Composition of Hydrido Complexes. Quantitative characterization of the equilibrium between [$HIr(CO)_3(PPh_3)$] and [$HIr(CO)_2(PPh_3)_2$] has been performed by in situ IR and NMR spectroscopy. Our approach was based on the variation of the partial pressure of carbon monoxide from ca. 3.9 MPa to approximately 10^{-2} MPa bar keeping the partial pressure of hydrogen constant at 1 MPa. This procedure was carried out with different ratios of [PPh_3]/[Ir] = 4, 10, and 20. For a representative illustration, in Figure 5, the infrared spectra for [PPh_3]/[Ir] = 4 are presented.

With the help of the software tool PCD,[33] pure component spectra and associated concentration profiles in dependence of the CO partial pressure have been extracted. Therefore, all spectra series (for the different ratios [PPh_3]/[Ir]) have been taken into account. From the analysis of the vibrational spectra,

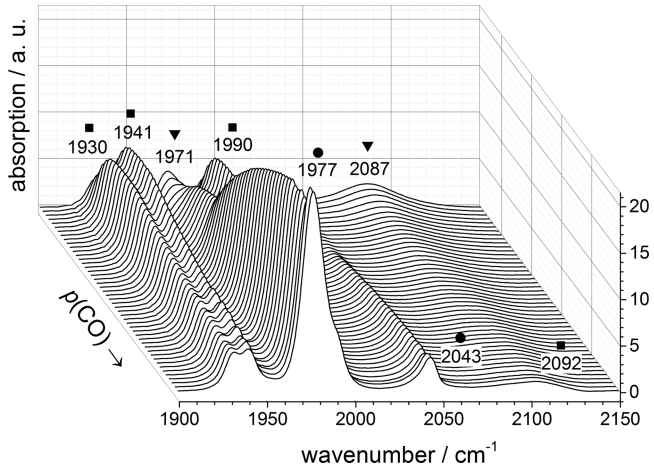

Figure 5. Infrared spectra series of a mixture of iridium hydrido complexes obtained by variation of the CO partial pressure in order to get a quantitative characterization of the respective equilibrium. Experimental conditions: [Ir] = 5.0 mM, [PPh_3] = 20 mM, θ = 100 °C, $p(CO)$ = 10^{-2} − 3.9 MPa, $p(H_2)$ = 1 MPa, solvent = toluene. ● ν(CO) = 1977, 2043 cm^{-1}: *a*-[$HIr(CO)_3(PPh_3)$]; ■ ν(CO) = 1930, 1941, 1980 (obsc.), 1990, 2092 cm^{-1}: *e,a*-[$HIr(CO)_2(PPh_3)_2$] and *e,e*-[$HIr(CO)_2(PPh_3)_2$]; ▼ ν(CO) = 1971, 2087 cm^{-1}: not attributable, but see below.

it is important to discuss a few points in more detail, see Figure 6.

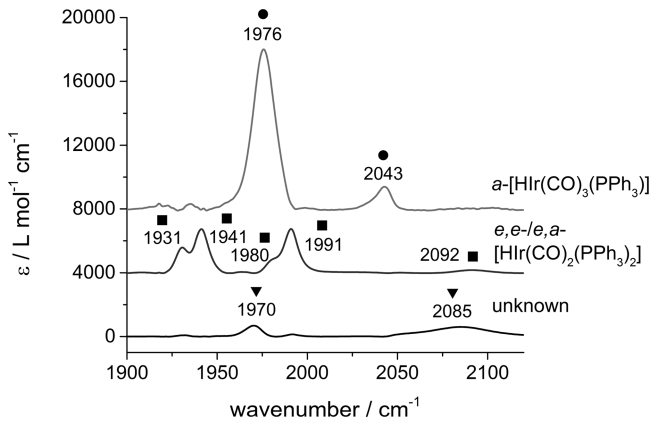

Figure 6. Pure component IR spectra from the treatment with the software tool PCD of spectra series taken from three experiments in which the CO partial pressure has been varied. Experimental conditions: [Ir] = 5.0 mM, [PPh_3] = 20, 50, 100 mM, θ = 100 °C, $p(CO)$ = 10^{-2} − 3.9 MPa, $p(H_2)$ = 1 MPa, solvent = toluene.

The molar absorption coefficients at band positions with the highest intensity are significantly different between the three components. That means that although a spectrum of a mixture shows only small intense bands for a specific component, this component can be present in significant molar concentrations when the respective molar absorption coefficients are small. This underlines that for a quantitative interpretation, the molar absorption coefficients should be accessible. On the other hand, such significant differences in the molar absorption coefficients may lead to large errors in the calculation of the concentration profiles, especially if vibrational bands overlap strongly as observed here. We estimated an error with respect to the initially applied iridium concentration of 2−10% for the

dx.doi.org/10.1021/cs500368z | ACS Catal. 2014, 4, 2097−2108

concentration profiles in the range of 3.9−0.5 MPa CO pressure (see further below).

Another point is that due to a fast equilibrium between the stereoisomers *e,e*-$[HIr(CO)_2(PPh_3)_2]$ and *e,a*-$[HIr(CO)_2(PPh_3)_2]$, the chemometric method only allowed us to obtain the corresponding infrared spectrum as a sum of both components. As a consequence, both complexes behave as a single component within the chemometric factorization.[18]

The last point concerns the third spectrum of a hitherto unknown species. We would like to mention that this spectrum differs from that of the monocarbonyl complex $[HIr(CO)(PPh_3)_3]$, which shows contributions at 1930 and 2073 cm^{-1} and which was expected to be part of the equilibrium composition at low CO partial pressures. It was found that by the reaction of *e,e*-/*e,a*-$[HIr(CO)_2(PPh_3)_2]$ with hydrogen, the same IR spectrum was recorded characterized by $\nu(CO)$ = 1971 and $\nu(Ir-H)$ = 2087 cm^{-1}. This compound was described in earlier studies and is presumably the trihydride complex $[H_3Ir(CO)(PPh_3)_2]$ (see Scheme 2a).[70−72] NMR spectroscopy

Scheme 2. (a) Reaction of Dicarbonyl Complexes *e,e*-/*e,a*-$[HIr(CO)_2(PPh_3)_2]$ with Hydrogen Yielding a Mixture of the Stereoisomeric Trihydride Complexes *fac-cis*- and *mer-trans*-$[H_3Ir(CO)(PPh_3)_2]$. (b) Conversion of *e,e,e*-$[HIr(CO)(PPh_3)_3]$ with Hydrogen Forms the Same Trihydride Complexes[a]

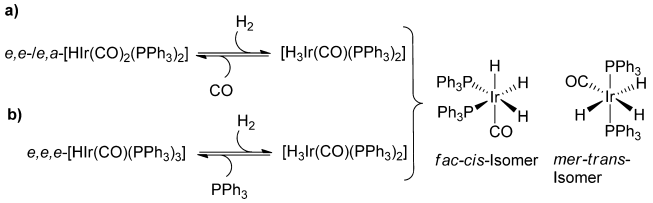

[a]For details of the reactions and a spectroscopic characterization, see the Supporting Information.

revealed that it is actually a mixture of *fac-cis*-$[H_3Ir(CO)(PPh_3)_2]$ and *mer-trans*-$[H_3Ir(CO)(PPh_3)_2]$. Interestingly, these trihydride complexes are also obtained when *e,e,e*-$[HIr(CO)(PPh_3)_3]$ was treated with molecular hydrogen.[70] For experimental and spectroscopic details, see the Supporting Information. The reaction in Scheme 2b is probably the reason why we could not detect *e,e,e*-$[HIr(CO)(PPh_3)_3]$ in these experiments. It can be concluded that the triphenylphosphine concentrations applied in this study are too low to shift the equilibrium toward detectable concentrations of hydridocarbonyl-tris(triphenylphosphine)iridium(I).

There are few reports about other iridium(III) trihydride complexes in the literature.[9,50,55,73,74] One example concerns $[H_3Ir(CO)_2(PPh_3)]$, which was characterized by Malatesta et al. This complex was not observed in our in situ FTIR experiments likely due to the applied elevated triphenylphosphine concentrations.[55]

In order to characterize the equilibrium of iridium complexes, we have to analyze the concentration profiles, see Figure 7. Such profiles were available by treatment of the spectral data with the PCD algorithm. Due to an overestimation, the molar fractions of the trihydrides were corrected so that they approach zero at higher CO partial pressures. This approach was based on the NMR spectroscopic investigation (see below). From the qualitative point of view, the dependency of the complex concentrations on the partial pressure or

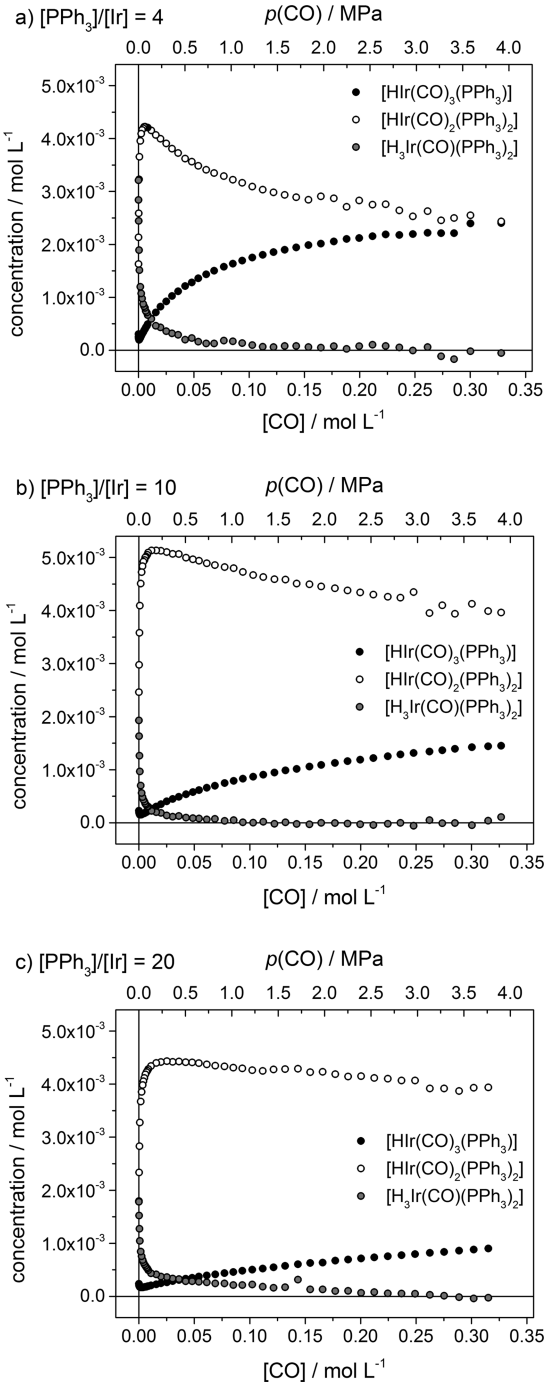

Figure 7. Concentration profiles resulting from the chemometric treatment (PCD) of spectra series acquired from experiments under varying partial pressures of carbon monoxide. Experimental conditions: [Ir] = 5.0 mM, $[PPh_3]$ = 20, 50, 100 mM, θ = 100 °C, $p(CO)$ = 10^{-2} − 3.9 MPa, $p(H_2)$ = 1 MPa, solvent = toluene. The error with respect to the initially applied iridium concentration in the range of 3.9−0.5 MPa was between ca. 2−10%.

concentration of carbon monoxide (solubility data for CO in toluene have been taken from the literature[75]) is comprehensible. At higher CO concentrations and lower triphenylphosphine concentrations (Figure 7a), ca. 50% of iridium is present as $[HIr(CO)_3(PPh_3)]$. The concentration of the latter is decreasing continuously with decreasing CO concentrations. With respect to the applied reaction conditions at 1.0 MPa carbon monoxide and 1.0 MPa hydrogen (Figure 4), for the

dx.doi.org/10.1021/cs500368z | ACS Catal. 2014, 4, 2097−2108

main components, the molar fraction of $[HIr(CO)_2(PPh_3)_2]$ is ca. 64%, and for $[HIr(CO)_3(PPh_3)]$, it is ca. 33%.

Higher triphenylphosphine concentrations resulted in lower $[HIr(CO)_3(PPh_3)]$ molar fractions and favored the formation of $[HIr(CO)_2(PPh_3)_2]$. Trihydride complexes are present at higher ratios of $p(H_2)/p(CO)$. Scheme 3 summarizes the investigated reaction sequence.

Scheme 3. Sequence of Equilibria Involving Triphenylphosphine-Modified Hydridocarbonyl Iridium Complexes

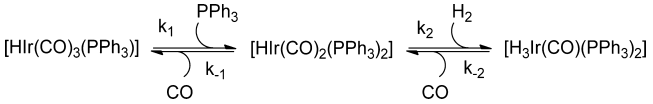

For a quantitative characterization, the following expression (eq 1) derived from a kinetic analysis is suitable (a kinetic derivation is shown in the Supporting Information).

$$K = \frac{k_1 k_2}{k_{-1} k_{-2}} = \frac{[H_3Ir(CO)(PPh_3)_2][CO]^2}{[HIr(CO)_3(PPh_3)][H_2][PPh_3]} \quad (1)$$

However, because of the fact that the trihydride complex is present in significant amounts only at larger ratios of $p(H_2)/p(CO)$ and due to numerical inaccuracies, it is more reliable to confine the characterization to the first partial reaction: $K_1 = k_1/k_{-1} = [CO][HIr(CO)_2(PPh_3)_2]/[PPh_3][HIr(CO)_3(PPh_3)]$. In the pressure range of 3.9−0.5 MPa, we estimated $K_1 \approx 7.3$ as an average value from all three experiments. We tried to obtain information about both connected reversible reactions also by a kinetic approach (see below).

The quantitative investigation of the equilibrium mixture under variation of the carbon monoxide partial pressure for $[PPh_3]/[Ir] = 4$ was carried out by NMR spectroscopy in a similar manner as used for IR investigations. [Ir(acac)(COD)] with a 4-fold molar excess of PPh_3 in toluene was subjected to a syngas atmosphere of varying composition at 100 °C (experimental details, see Supporting Information). The composition of the solution was examined in situ with ^1H and ^{31}P NMR.

The generation of the hydrido−carbonyl complexes from the cyclooctadiene precursor complex occurred stepwise at 100 °C. Eventually, a mixture of $[HIr(CO)_2(PPh_3)_2]$ and $[HIr(CO)_3(PPh_3)]$ was observed. When the partial pressure of CO was changed (keeping $p(H_2)$ constant at 1 MPa), the molar ratio of these two compounds changed according to the expectation and in a similar manner as observed by IR spectroscopy. Due to limitations imposed by measurement sensitivity and experiment time, a detailed kinetic or thermodynamic interpretation is not possible. However, this experiment provides a clear proof that, at low partial pressure of CO and hydrogen excess, Ir(III) trihydrides rather than $[HIr(CO)(PPh_3)_3]$ are formed (Figure 8). This is evident from both ^1H and ^{31}P NMR spectra. The chemical shift $\delta(^{31}P)$ for $[HIr(CO)(PPh_3)_3]$ is 15.2 ppm, which is not observed under these conditions.

Such trihydrides can also be easily prepared from $[HIr(CO)(PPh_3)_3]$ or $[HIr(CO)_2(PPh_3)_2]$ under hydrogen pressure (Scheme 2). Their stability is sufficient for a spectroscopic characterization even after release of the pressure. This allows a direct comparison and reliable identification of the compounds under reaction conditions, see Figure 8.

We have shown that for the applied conditions, the spectroscopically measurable resting state is a mixture of *a*-$[HIr(CO)_3(PPh_3)]$, *e,e/e,a*-$[HIr(CO)_2(PPh_3)_2]$, and *fac-cis/mer-trans*-$[H_3Ir(CO)(PPh_3)_2]$ (see Figure 4). The molar concentrations of the iridium complexes have been determined. Those molar concentrations did depend on the exact reaction conditions. A correlation between the reaction conditions, the composition of iridium complexes, and the catalytic activity is obvious. For example, it has been shown in the literature[9] that an excess of CO suppresses the hydrogenation of the substrate. Furthermore, the concentration of triphenylphosphine had a significant effect on the reaction rate. A systematic study of the reaction kinetics in combination with operando spectroscopic

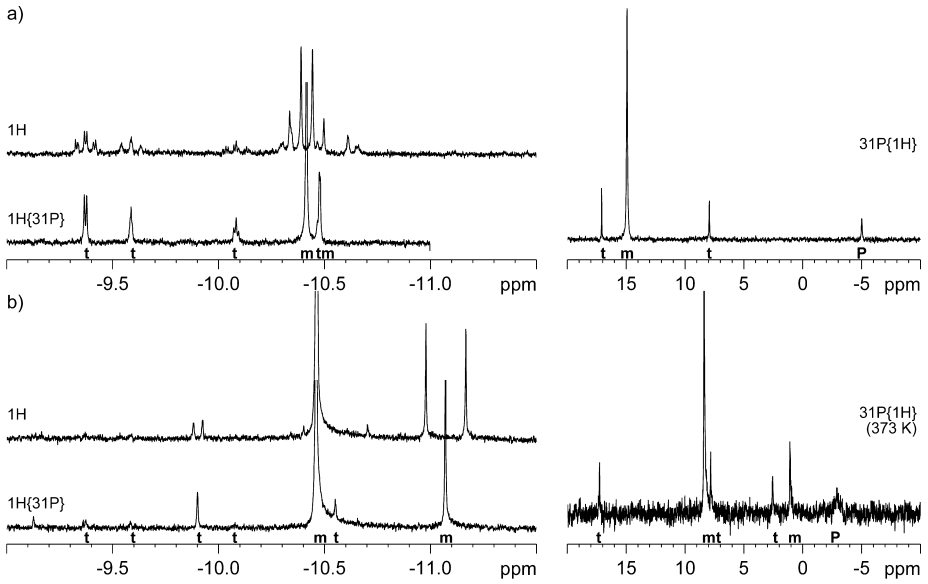

Figure 8. ^1H and $^{31}P\{^1H\}$ NMR spectra of Ir carbonyl−hydrido complexes. (a) $[HIr(CO)(PPh_3)_3]$ treated with 1.0 MPa H_2 at 100 °C. (b) Spectra taken in situ during the experiment described in the text: $p(H_2) = 1.01$ MPa, $p(CO) = 0.01$ MPa. The letter t designates Ir(III) trihydrido complexes, m designates Ir(I) monohydrido complexes, and P represents free PPh_3. Solvent = toluene.

dx.doi.org/10.1021/cs500368z | ACS Catal. 2014, 4, 2097−2108

measurements could indeed reveal such correlations. However, such an investigation goes beyond the subject of the present study.

Estimation of Rate Constants. We were further interested to determine the single rate constants of the reaction sequence (Scheme 3) in order to obtain a deeper insight into such equilibria between iridium complexes. We took advantage of the fact that both partial reactions can be treated separately from the experimental point of view.

First, we were investigating the partial reaction between $[HIr(CO)_3(PPh_3)]$, $[HIr(CO)_2(PPh_3)_2]$, carbon monoxide, and triphenylphosphine (see Scheme 4).

Scheme 4. Partial Equilibrium Reaction between Tricarbonyl Complex $[HIr(CO)_3(PPh_3)]$, Dicarbonyl Complex $[HIr(CO)_2(PPh_3)_2]$, Carbon Monoxide, and Triphenylphosphine

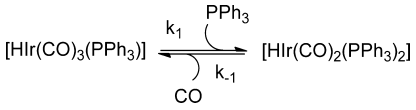

Taking into consideration that we cannot precisely study fast reactions with our FTIR apparatus we decided to investigate the reaction at lower temperatures and used a stopped-flow unit coupled with a FTIR spectrometer capable of measuring in the rapid-scan mode. Details for the stopped-flow setup are given in the Experimental Section. We prepared a solution of a mixture of $[HIr(CO)_3(PPh_3)]$ and $[HIr(CO)_2(PPh_3)_2]$ with an iridium concentration of 10.06 mM and an initial triphenylphosphine concentration of 20.11 mM. After formation of the iridium complexes from [(acac)Ir(COD)] at 100 °C, $p(CO)$ = 1 MPa, and $p(H_2)$ = 1 MPa, the solution was cooled to 30 °C. Partial pressures were set to $p(CO)$ = 4 MPa and $p(H_2)$ = 0.5 MPa to achieve a ratio of $p(CO)/p(H_2)$ = 8 and thus to exclude the formation of trihydrides. Then the pressure was reduced to the ambient value. The concentrations of carbon monoxide and hydrogen of the gas-saturated solutions were determined from the partial pressures as $[CO]$ = 8.1 mM[75] (0.086 MPa) and $[H_2]$ = 0.3 mM[76] (0.011 MPa). This solution was used for the first channel of the stopped-flow unit. An additional solution of triphenylphosphine, $[PPh_3]$ = 80.84 mM, which was also saturated with CO, was provided for the second channel. The concentration was selected so that after injecting equal volumina of both solutions to the stopped-flow cell, the concentration of $[PPh_3]$ was 50.47 mM and the iridium concentration was 5.03 mM, resulting in a ratio of $[PPh_3]/[Ir]$ = 10. The reaction led to a conversion of $[HIr(CO)_3(PPh_3)]$ into $[HIr(CO)_2(PPh_3)_2]$ and carbon monoxide. The initial composition of the iridium complexes were concn $[HIr(CO)_3(PPh_3)]$ = 0.74 mM and concn $[HIr(CO)_2(PPh_3)_2]$ = 4.29 mM.

Figure 9 shows the concentration of $[HIr(CO)_3(PPh_3)]$ based on intensity ratios between Int. $[HIr(CO)_3(PPh_3)]$ for $\nu(CO)$ = 1977.3 cm^{-1} and Int. $[HIr(CO)_2(PPh_3)_2]$ for $\nu(CO)$ = 1989.8 cm^{-1} versus time. Precedingly determined absorption coefficients have been used for calculating the concentration from intensity ratios. From the concentration data, the extent of reaction x has been calculated and used for further analysis.

At this point, we would like to outline the steps for how to access to the single rate constants in Scheme 4.[77] A complete derivation can be found in the Supporting Information. Because

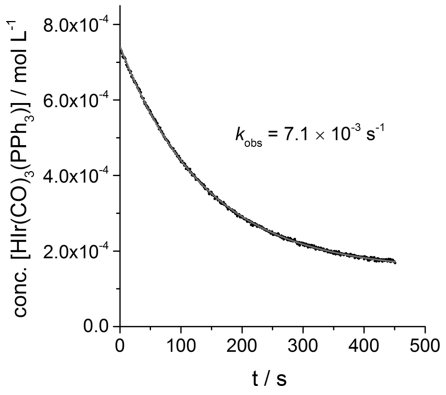

Figure 9. Molar concentration vs time of the iridium complex $[HIr(CO)_3(PPh_3)]$ during the stopped-flow experiment at 30 °C. The fit-function used was $y = a(1 - exp(k_{obs}t)) + b$.

both reaction steps are stoichiometrically dependent, only one extent of the reaction is needed for the kinetic treatment. Starting from eq 2, one gets eq 3 after expansion, where x_∞ is the value of x at equilibrium and x_u is the second zero which has no physical meaning. The value of x_∞ is to be determined from the experiment, and x_u can be calculated by Vieta's formulas. The value Δk is composed with $\Delta k = k_1 - k_{-1}$.

$$\frac{dx}{t} = k_1([A]_0 - x)([B]_0 - x) - k_{-1}([C]_0 + x)([D]_0 + x) \quad (2)$$

$$\frac{dx}{t} = \Delta k(x - x_\infty)(x - x_u) \quad (3)$$

After separation of the variables and integration, eq 4 is obtained. The slope from a plot of $\ln((x - x_\infty)/(x - x_u))/(x_\infty - x_u)$ versus time gives Δk, and with the help of the equilibrium constant, the single rate constants can be calculated.

$$\frac{\ln\left(\frac{x - x_\infty}{x - x_u}\right)}{(x_\infty - x_u)} = \Delta kt \quad (4)$$

We performed this experiment also at 35 and 40 °C in order to use the activation energy based on the simple Arrhenius equation for estimation of the rate constants at 100 °C. Due to technical reasons, experiments at higher temperatures could not be performed with the stopped-flow apparatus. We conducted a repetition experiment at each temperature. Results are given in Table 1.

The second partial reaction (Scheme 5) of the sequence depicted in Scheme 3 was treated slightly different, because it was not possible to set higher pressures/concentrations of hydrogen with the stopped-flow apparatus. Because it was found during preliminary experiments that the second partial reaction starting from $[HIr(CO)_2(PPh_3)_2]$ was comparably slow, this reaction could be studied with the conventional FTIR setup.

We took advantage of the fact that $[HIr(CO)_2(PPh_3)_2]$ (equilibrium mixture consisting of *e,e*- and *e,a*-isomer) can be prepared easily in solution and used it as a starting material. The solution with a concentration of $[(HIr(CO)_2(PPh_3)_2)]$ = 4.99 mM was free of the dissolved gases carbon monoxide and hydrogen after removing them by flushing the solution with an argon stream. At reaction temperature, 1 MPa (30.0 mM)[76] of hydrogen was added. The basis for the kinetic analysis was the concentration profile of $[HIr(CO)_2(PPh_3)_2]$. Concentrations

dx.doi.org/10.1021/cs500368z | ACS Catal. 2014, 4, 2097−2108

Table 1. Single Rate Constants for Partial Reactions (Schemes 4 and 5)

T (K)	k_1 (L mol^{-1} s^{-1})	k_{-1} (L mol^{-1} s^{-1})	k_2 (L mol^{-1} s^{-1})	k_{-2} (L mol^{-1} s^{-1})
303.15	0.170	0.021	0.053	0.207
308.15	0.189	0.029	0.088	0.268
313.15	0.218	0.030	0.136	0.417
(373.15)	(0.731)	(0.178)	(14.0)	(12.1)
$E_{a,obs}$ (kJ mol^{-1})	19.7	28.1	74.9	55.1

Scheme 5. Partial Equilibrium Reaction Involving $[HIr(CO)_2(PPh_3)_2]$, $[H_3Ir(CO)(PPh_3)_2]$, Carbon Monoxide, and Hydrogen

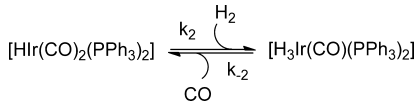

were calculated with the help of determined absorption coefficients. The procedure for the determination of the rate constants k_2 and k_{-2} is identical to that described above (see Table 1 for results).

From this data, it can be concluded that for the first partial reaction the rate of the forward reaction is higher than the reverse reaction. The ratio of k_1/k_{-1} changes from ca. 8.1 at 303.15 K to 4.1 at 373.15 K. The extrapolation to 373.15 K is uncertain due to the limited experimental data; therefore, values are in brackets. The equilibrium constant found in the CO variation experiment with $k_1/k_{-1} \approx 7.3$ is in good agreement with these results. With respect to the second partial reaction, the rate of the addition of hydrogen to $[HIr(CO)_2(PPh_3)_2]$ is slower in comparison to that of the addition of CO to $[H_3Ir(CO)(PPh_3)_2]$. The ratio of k_2/k_{-2} at 303.15 K is 0.25, and at 373.15 K, it is 1.1 due to the difference in activation energies. With this, we can calculate the overall equilibrium constant $K = k_1k_2/k_{-1}k_{-2}$ with ca. 2.1 for 303.15 K and 4.8 for 373.15 K.

Quantification of the Molar Fractions of *e,e*-$[HIr(CO)_2(PPh_3)_2]$ and *e,a*-$[HIr(CO)_2(PPh_3)_2]$. So far we could not determine the molar fractions of the stereoisomers *e,e*-$[HIr(CO)_2(PPh_3)_2]$ and *e,a*-$[HIr(CO)_2(PPh_3)_2]$. Both complexes are in equilibrium with each other which must be relatively fast (see Scheme 6).[58,64] By means of ^{1}H and ^{31}P{^{1}H} NMR spectroscopy, we only observed one set of signals at room temperature. The infrared spectrum shows bands of both complexes. However, because the experimental absorption coefficients are not known, we cannot analyze it directly in a quantitative manner. In order to investigate the equilibrium composition quantitatively for a broad temperature range, we performed variable temperature IR and NMR spectroscopy experiments.

Scheme 6. Equilibrium of the Interconversion of Two Stereoisomeric Forms of Hydridodicarbonylbis(triphenylphosphine)iridium(I)

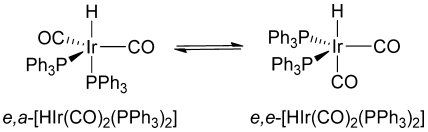

e,a-$[HIr(CO)_2(PPh_3)_2]$ *e,e*-$[HIr(CO)_2(PPh_3)_2]$

For the IR experiment, we have used a variable-temperature cell holder from Specac with a sealed liquid transmission cell (path length = 0.1 mm). We applied a solution of a mixture of both stereoisomeric hydrido complexes with [Ir] = 5.0 mM and $[PPh_3]$ = 50.1 mM at ambient pressure. The spectrum showed only bands of both complexes *e,e*-$[HIr(CO)_2(PPh_3)_2]$ and *e,a*-$[HIr(CO)_2(PPh_3)_2]$ (see Figure 10). We varied the temperature between 193−363 K (−80 to 90 °C) in 10 K intervals.

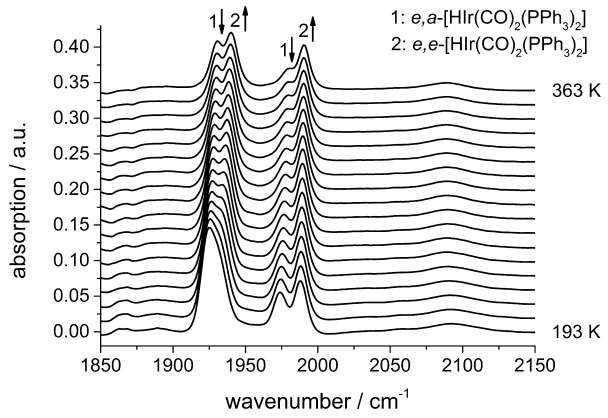

Figure 10. Experimentally registered spectra from a mixture of *e,a*-$[HIr(CO)_2(PPh_3)_2]$ and *e,e*-$[HIr(CO)_2(PPh_3)_2]$ for the temperature range of 193−363 K. Contributions at 303 K are *e,a*-isomer: ν(CO) = 1929, 1978 cm^{-1}; *e,e*-isomer: ν(CO) = 1938, 1990 cm^{-1}.

The band intensities from the *e,e*-isomer relative to those of the *e,a*-isomer are increasing with higher temperature. Band intensities and frequency positions varied with the temperature so that a quantitative analysis of the spectroscopic data can only be performed on relative band intensities. As an approach for quantification, we used the intensity ratio from DFT-calculated vibrational spectra as a reference point. Intensities from the experimental spectra were calculated via curve fitting using the implemented program in the Bruker OPUS 7.0 software. Figure 11a illustrates the molar fractions of the *e,e*-isomer at the adjusted temperatures. From that data, equilibrium constants have been calculated from which a value for the Gibbs free energy could be estimated with ca. 2.16 kJ mol^{-1} (Figure 11b).

We studied the equilibrium composition of both hydrido−dicarbonylbis(triphenylphosphine)iridium(I) complexes also by NMR spectroscopy. Although the iridium dicarbonyl complex must be prepared under synthesis gas pressure, it is sufficiently stable under an inert gas atmosphere in the NMR tube to allow further characterization. The *e,a*- and *e,e*-isomers interconvert quickly at room temperature (Scheme 6), so only one set of signals is present in the ^{1}H and ^{31}P{^{1}H} NMR spectra, but the latter exhibited a broad resonance line. Upon cooling, further broadening and decoalescence occurred (Figure 12). For the ^{1}H NMR spectra, this phenomenon has already been described.[58,64] The phosphorus spectra provide as additional information that one of the stereoisomers undergoes further molecular dynamics, and its signal at 4 ppm broadens again when cooling from 217 K/−56 °C to 202 K/−71 °C. Because

dx.doi.org/10.1021/cs500368z | ACS Catal. 2014, 4, 2097−2108

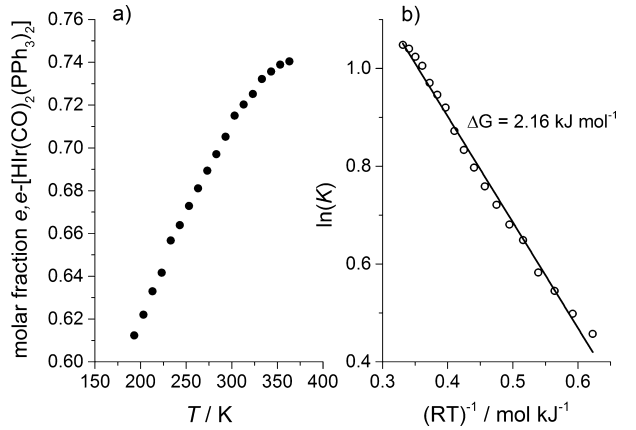

Figure 11. (a) Molar fractions of the bisequatorial isomer *e,e*-$[HIr(CO)_2(PPh_3)_2]$ from a variable-temperature IR spectroscopic experiment. (b) From the analysis of the respective equilibrium constants in dependence of the temperature, a value for the Gibbs free energy of the complex equilibrium could be calculated.

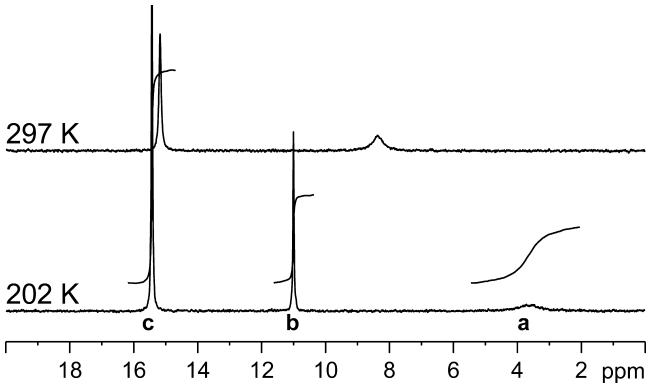

Figure 12. $^{31}P\{^1H\}$ NMR spectra of the iridium dicarbonyl complex in toluene, at 297 K/24 °C (top trace) and 202 K/−71 °C (bottom trace); **a** represents the *e,a*-isomer, **b** the *e,e*-isomer, and **c** $[HIr(CO)(PPh_3)_3]$. Further conditions: [Ir] = 5.0 mM, $[PPh_3]$ = 150 mM, solvent = toluene-d_8.

the *e,a*-isomer should exhibit inequivalent P atoms in the slow exchange regime, it is reasonable to assume that it is represented by this broad resonance. The proton NMR spectra (see literature[58] and Supporting Information) are in line with this interpretation. At 202 K/−71 °C, we observed *two* triplets ($^2J_{P,H}$ 18 and 36 Hz) rather than the expected one triplet and one double doublet (for the *e,a*-isomer with two different coupling constants). Most likely, the 36 Hz represent an averaged value for the *cis* and the *trans* coupling. On the basis of this assignment, an equilibrium fraction of 0.62 for *e,e*-$[HIr(CO)_2(PPh_3)_2]$ and 0.38 for *e,a*-$[HIr(CO)_2(Ph_3)_2]$ can be estimated at 202 K/−71 °C (*cf.* Figure 12). For the rhodium analogue, a molar fraction of 0.85 for *e,e*-$[HRh(CO)_2(PPh_3)_2]$ and 0.15 for *e,a*-$[HRh(CO)_2(PPh_3)_2]$ was determined at low temperatures.[78]

Because of said chemical exchange and signal averaging, the molar fractions as a function of the temperature cannot be determined by varying the measurement temperature. Yagupsky and Wilkinson[58] proposed the averaged coupling constant $^2J_{P,H}$ as a potential indicator for the equilibrium position, and we are currently exploring the usability of this approach.

It should be noted that $[HIr(CO)(PPh_3)_3]$ does not exhibit molecular dynamics in toluene solution. Upon cooling, no changing NMR lineshapes are observed.

CONCLUSION

In this study, we have presented an extended quantitative characterization of a mixture of phosphine-modified iridium complexes applied as catalysts in the hydroformylation of alkenes. FTIR spectra could be well interpreted, supported by results from NMR measurements, DFT calculations, and deuteration experiments. It was found that at common reaction conditions, the complex $[HIr(CO)(PPh_3)_3]$ is not part of the catalyst mixture. At higher $p(H_2)/p(CO)$ ratios, a mixture of trihydride complexes are formed in significant molar fractions. The corresponding sequence of equilibrium reactions involving all observable iridium complexes, carbon monoxide, triphenylphosphine, and hydrogen could be studied experimentally and characterized by kinetic parameters. FTIR spectroscopic data were treated by chemometric methods. Even the single rate constants of both relevant partial reactions could be determined. For that purpose, stopped-flow experiments gave access to the rate constants of the faster partial reaction. The temperature dependence of the equilibrium between the stereoisomers *e,e*-$[HIr(CO)_2(PPh_3)]$ and *e,a*-$[HIr(CO)_2(PPh_3)]$ was studied in the range of −80 to 90 °C using a variable-temperature unit for FTIR measurements. As evidenced in this study, especially the combination of different experimental/analytical tools and approaches can contribute substantially to a detailed characterization of a mixture of homogeneous catalysts active in the hydroformylation reaction. The results represent a sound basis for further operando spectroscopic studies where the influence of reactant concentrations on the kinetics of the hydroformylation and composition of iridium complexes are correlated.

EXPERIMENTAL SECTION

Materials. Toluene (Acros, >99.8%) has been dried via distillation over sodium and stored under argon. *n*-Hexane (Sigma-Aldrich, >99%) was distilled over Sicapent (Merck) and stored under argon. Dodecane (Sigma-Aldrich, >99%) which was used as internal GC-standard was dried by storage over Sicapent for 1 week and distilled after separation of the drying agent and stored under argon. 3,3-Dimethyl-1-butene, >99% (GC), (Sigma-Aldrich, 95%) were distilled over sodium and stored under argon.

Further chemicals used in the present study: 1,5-cyclooctadiene(acetylacetonato)iridium(I) (99% Strem), hydridocarbonyltris(triphenylphosphine)iridium(I) (99% Strem), triphenylphosphine (99% Sigma-Aldrich), diphenyl carbonate (used as internal standard for FTIR measurements, 99% Sigma-Aldrich). Gases used in this study: synthesis gas (CO/H_2 = 1:1, from carbon monoxide 99.997% and hydrogen 99.999%, Linde), carbon monoxide (99.997%, Linde), hydrogen (99.9993%, Linde), deuterium (99.9%, Linde), and argon (99.999%, Linde).

Devices and Procedures. Reactions for in situ infrared spectroscopic analysis were performed in a HP-FTIR apparatus consisting of a 200 mL stainless steel autoclave with a gas entrainment impeller and an oil bath thermostat (premex reactor AG, Leimen, Germany) equipped with a pressurizable and heatable transmission flow-through IR cell (Dr. Bastian Feinwerktechnik GmbH, Wuppertal, Germany) and an

dx.doi.org/10.1021/cs500368z | ACS Catal. 2014, 4, 2097−2108

automated sampling device for taking GC samples during the reaction (amplius GmbH, Rostock, Germany).

Transport of the liquid reaction solution through the IR cell and back to the autoclave was realized by a micro gear pump (mzr-7255, HNP Mikrosysteme GmbH, Parchim, Germany). A syringe pump (PHD Ultra 4400, Harvard Apparatus GmbH, March-Hugstetten, Germany) with a 8 mL syringe made of stainless steel has been used for olefin injection. For the infrared spectroscopic measurements, a Bruker Tensor 27 FTIR spectrometer with a MCT-A detector was used. CaF_2 (Korth Kristalle GmbH, Kiel, Germany) was used as window material. The optical path length was 0.1 mm. Pressurization facilities were installed for synthesis gas (CO/H_2 = 1:1) as well as carbon monoxide, hydrogen, and deuterium. For regulation of the consumed gas (CO/H_2 = 1:1) and keeping the pressure constant during the hydroformylation reaction, a pressure controller (Brooks Instrument, Hatfield, PA, U.S.A) was used. A scheme of the HP-FTIR apparatus can be found elsewhere.[35]

Solutions were prepared from the solids using standard Schlenk techniques. All liquid components have been transferred into the autoclave via standard Schlenk techniques. The speed chosen for the micro gear pump was 2333 rpm (displacement volume = 48 μL). The residence time in the periphery between the autoclave and IR cell was ca. 5 s. However, because the entire mixing process after adding a reactant to the system is significantly longer,[19] we considered a mixing time of about 100−120 s. The stirrer speed was set to 600 rpm.

Hydroformylation Reaction. All solutions except the olefin were transferred into the autoclave. The solution was heated to 100 °C. Then the system was pressurized with 0.9 MPa of carbon monoxide, and 0.9 MPa of hydrogen was added. This was taken as the start of the preformation period in order to form the hydrido complexes from the precursor and triphenylphosphine. This was coupled with an in situ FTIR measurement which allowed observation of the status when the preformation reaction was accomplished. After that, the olefin was injected with the help of the syringe pump. Partial pressures were set to 1 MPa of carbon monoxide and 1 MPa of hydrogen. The olefin injection was taken as the reaction start.

FTIR spectra were recorded between 3950 and 700 cm^{-1} with a spectral resolution of 2 cm^{-1}. Ten scans were collected per FTIR spectrum (double-sided, forward−backward). The mirror speed was set to 40 kHz.

Gas chromatographic analyses have been performed with a 7890 A GC System from Agilent Technologies with a Petrocol DH 150 column (Supelco, Inc.).

Stopped-Flow Experiments. The time-resolved infrared experiments have been carried out on a stopped-flow unit (TgK Scientific, U.K.) combined with a VERTEX 80 (Bruker) with rapid-scan extension. The solutions and the IR cell have been thermostated before and during the reaction. The IR cell has CaF_2-windows. The optical path length was specified by the supplier with 100 μm. The spectra (16 scans per spectrum) were taken with a resolution of 2 cm^{-1}.

High-Pressure NMR Experiments. NMR spectra were collected on a Bruker Avance 400 spectrometer using a high-pressure gas flow cell connected to devices allowing for continuous gas supply and the control of gas flow and pressure.[79]

Computational Details. Geometry optimizations and frequency calculations have been performed with the Turbomole V6.3.1 program package.[80] DFT calculations were carried out using the BP86[81] functional and def-SV(P)[82] basis set on all atoms. No scaling factor has been applied to the calculated frequencies.

■ ASSOCIATED CONTENT

Supporting Information

Detailed description of experiments, experimental FTIR spectra of hydrido and deuterido complexes, vibrational spectra calculated by DFT methods, characterization of complexes by NMR spectroscopy, derivation of kinetic expressions, geometries from DFT calculations. This material is available free of charge via the Internet at http://pubs.acs.org.

■ AUTHOR INFORMATION

Corresponding Authors

*E-mail: christoph.kubis@catalysis.de.

*E-mail: armin.boerner@catalysis.de.

Notes

The authors declare no competing financial interest.

■ ACKNOWLEDGMENTS

This work was financially supported by the Bundesministerium für Bildung und Forschung (Federal Ministry of Education and Research) within the PROFORMING project (no. 03X3559). We thank Dr. Koichi Fumino for assistance during the variable-temperature FTIR measurements and Anja König for helpful discussions.

■ REFERENCES

(1) *Rhodium Catalyzed Hydroformylation*; van Leeuwen, P. W. N. M., Claver, C., Eds.; Kluwer: Dordrecht, The Netherlands, 2000.

(2) (a) Bohnen, H.-W.; Cornils, B. *Adv. Catal.* **2002**, *47*, 1−64. (b) Frohning, C. D.; Kohlpaintner, C. W.; Bohnen, H.-W. In *Applied Homogeneous Catalysis with Organometallic Compounds*, 2nd ed.; Cornils, B., Herrmann, W. A., Eds.; Wiley-VCH: Weinheim, Germany, 2002; pp 31−103.

(3) Wiese, K.-D.; Obst, D. In *Topics in Organometallic Chemistry*; Beller, M., Ed.; Springer: Berlin, Heidelberg, Germany, Vol. *18*, 2006; pp 1−34.

(4) (a) Franke, R.; Selent, D.; Börner, A. *Chem. Rev.* **2012**, *112*, 5675−5732. (b) Gusevskaya, E. V.; Jiménez-Pinto, J.; Börner, A. *ChemCatChem.* **2014**, *6*, 382−411.

(5) Pospech, J.; Fleischer, I.; Franke, R.; Buchholz, S.; Beller, M. *Angew. Chem., Int. Ed.* **2013**, *52*, 2852−2872.

(6) Konya, D.; Almeida Leñero, K. Q.; Drent, E. *Organometallics* **2006**, *25*, 3166−3174.

(7) Jennerjahn, R.; Piras, I.; Jackstell, R.; Franke, R.; Wiese, K.-D.; Beller, M. *Chem.—Eur. J.* **2009**, *15*, 6383−6388.

(8) Moreno, M. A.; Haukka, M.; Pakkanen, T. A. *J. Catal.* **2003**, *215*, 326−331.

(9) Piras, I.; Jennerjahn, R.; Jackstell, R.; Spannenberg, A.; Franke, R.; Beller, M. *Angew. Chem., Int. Ed.* **2011**, *50*, 280−284.

(10) Rosales, M.; Alvarado, B.; Arrieta, F.; De La Cruz, C.; González, Á.; Molina, K.; Soto, O.; Salazar, Y. *Polyhedron* **2008**, *27*, 530−536.

(11) Takahashi, K.; Yamashita, M.; Tanaka, Y.; Nozaki, K. *Angew. Chem.* **2012**, *124*, 4459−4463.

(12) Takahashi, K.; Yamashita, M.; Nozaki, K. *J. Am. Chem. Soc.* **2012**, *134*, 18746−18757.

(13) Fleischer, I.; Wu, L.; Profir, I.; Jackstell, R.; Franke, R.; Beller, M. *Chem.—Eur. J.* **2013**, *19*, 10589−10594.

(14) Wu, L.; Fleischer, I.; Jackstell, R.; Profir, I.; Franke, R.; Beller, M. *J. Am. Chem. Soc.* **2013**, *135*, 14306−14312.

(15) (a) *Mechanisms in Homogeneous Catalysis*; Heaton, B., Ed.; Wiley-VCH: Weinheim, Germany, 2005. (b) Dwyer, C.; Assumption, H.; Coetzee, J.; Crause, C.; Damoense, L.; Kirk, M. *Coord. Chem. Rev.* **2004**, *248*, 653−669. (c) Damoense, L.; Datt, M.; Green, M.;

Steenkamp, C. *Coord. Chem. Rev.* **2004**, *248*, 2393−2407. (d) Kamer, P. C. J.; van Rooy, A.; Schoemaker, G. C.; van Leeuwen, P. W. N. M. *Coord. Chem. Rev.* **2004**, *248*, 2409−2424. (e) Lazzaroni, R.; Settambolo, R.; Alagona, G.; Gio, C. *Coord. Chem. Rev.* **2010**, *254*, 696−706.
(16) Diebolt, O.; van Leeuwen, P. W. N. M.; Kamer, P. C. J. *ACS Catal.* **2012**, *2*, 2357−2370.
(17) Malinowski, E.: *Factor Analysis in Chemistry*; Wiley: New York, 2002.
(18) Maeder, M.; Neuhold, Y.-M.: *Practical Data Analysis in Chemistry*; Elsevier: Amsterdam, The Netherlands, 2007.
(19) Garland, M. In *Mechanisms in Homogeneous Catalysis*; Heaton, B.; Ed.; Wiley-VCH: Weinheim, Germany, 2005; pp 151−193.
(20) Garland, M.; Li, C.; Guo, L. *ACS Catal.* **2012**, *2*, 2327−2334.
(21) Chew, W.; Widjaja, E.; Garland, M. *Organometallics* **2002**, *21*, 1982−1990.
(22) Widjaja, E.; Li, C.; Garland, M. *Organometallics* **2002**, *21*, 1991−1997.
(23) Widjaja, E.; Li, C.; Chew, W.; Garland, M. *Anal. Chem.* **2003**, *75*, 4499−4507.
(24) Li, C.; Widjaja, E.; Garland, M. *J. Catal.* **2003**, *213*, 126−134.
(25) Li, C.; Widjaja, E.; Chew, W.; Garland, M. *Angew. Chem., Int. Ed.* **2002**, *41*, 3785−3789.
(26) Li, C.; Widjaja, E.; Garland, M. *J. Am. Chem. Soc.* **2003**, *125*, 5540−5548.
(27) Li, C.; Widjaja, E.; Garland, M. *Organometallics* **2004**, *23*, 4131−4138.
(28) Liu, G.; Li, C.; Guo, L.; Garland, M. *J. Catal.* **2006**, *237*, 67−78.
(29) Li, C.; Chen, L.; Garland, M. *J. Am. Chem. Soc.* **2007**, *129*, 13327−13334.
(30) Li, C.; Chen, L.; Garland, M. *Adv. Synth. Catal.* **2008**, *350*, 679−690.
(31) Li, C.; Cheng, S.; Tjahjono, M.; Schreyer, M.; Garland, M. *J. Am. Chem. Soc.* **2010**, *132*, 4589−4599.
(32) Li, C.; Gao, F.; Cheng, S.; Tjahjono, M.; van Meurs, M.; Ying Tay, B.; Jacob, C.; Guo, L.; Garland, M. *Organometallics* **2011**, *30*, 4292−4296.
(33) Neymeyr, K.; Sawall, M.; Hess, D. *J. Chemometrics* **2010**, *24*, 67−74.
(34) Kubis, C.; Ludwig, R.; Sawall, M.; Neymeyr, K.; Börner, A.; Wiese, K.-D.; Hess, D.; Franke, R.; Selent, D. *ChemCatChem.* **2010**, *2*, 287−295.
(35) Kubis, C.; Selent, D.; Sawall, M.; Ludwig, R.; Neymeyr, K.; Baumann, W.; Franke, R.; Börner, A. *Chem.—Eur. J.* **2012**, *18*, 8780−8794.
(36) Sawall, M.; Börner, A.; Kubis, C.; Selent, D.; Ludwig, R.; Neymeyr, K. *J. Chemometrics* **2012**, *26*, 538−548.
(37) Fischer, C.; Schulz, S.; Drexler, H.-J.; Selle, C.; Lotz, M.; Sawall, M.; Neymeyr, K.; Heller, D. *ChemCatChem.* **2012**, *4*, 81−88.
(38) Gärtner, F.; Boddien, A.; Barsch, E.; Fumino, K.; Losse, S.; Junge, H.; Hollmann, D.; Brückner, A.; Ludwig, R.; Beller, M. *Chem.—Eur. J.* **2011**, *17*, 6425−6436.
(39) Allian, A. D.; Wang, Y.; Saeys, M.; Kuramshina, G. M.; Garland, M. *Vib. Spectrosc.* **2006**, *41*, 101−111.
(40) Allian, A. D.; Tjahjono, M.; Garland, M. *Organometallics* **2006**, *25*, 2182−2188.
(41) Christiansen, A.; Li, C.; Garland, M.; Selent, D.; Ludwig, R.; Franke, R.; Börner, A. *ChemCatChem.* **2010**, *2*, 1278−1285.
(42) Christiansen, A.; Li, C.; Garland, M.; Selent, D.; Ludwig, R.; Spannenberg, A.; Baumann, W.; Franke, R.; Börner, A. *Eur. J. Org. Chem.* **2010**, 2733−2741.
(43) Boddien, A.; Loges, B.; Gärtner, F.; Torborg, C.; Fumino, K.; Junge, H.; Ludwig, R.; Beller, M. *J. Am. Chem. Soc.* **2010**, *132*, 8924−8934.
(44) Hess, D.; Hannebauer, B.; König, M.; Reckers, M.; Buchholz, S.; Franke, R. *Z. Naturforsch.* **2012**, *67b*, 1061−1069.
(45) Yagupsky, G.; Brown, C. K.; Wilkinson, G. *J. Chem. Soc. D: Chem. Commun.* **1969**, 1244−1245.
(46) Yagupsky, G.; Brown, C. K.; Wilkinson, G. *J. Chem. Soc. A* **1970**, 1392−1401.
(47) Deutsch, P. P.; Eisenberg, R. *Organometallics* **1990**, *9*, 709−718.
(48) Permin, A. B.; Eisenberg, R. *J. Am. Chem. Soc.* **2002**, *124*, 12406−12407.
(49) Godard, C.; Duckett, S. B.; Henry, C.; Polas, S.; Toose, R.; Whitwood, A. C. *Chem. Commun.* **2004**, 1826−1827.
(50) Fox, D. J.; Duckett, S. B.; Flaschenriem, C.; Brennessel, W. W.; Schneider, J.; Gunay, A.; Eisenberg, R. *Inorg. Chem.* **2006**, *45*, 7197−7209.
(51) Rosales, M.; González, A.; Guerrero, Y.; Pacheco, I.; Sánchez-Delgado, R. A. *J. Mol. Catal. A* **2007**, *270*, 241−249.
(52) Casey, C. P.; Whiteker, G. T.; Melville, M. G.; Petrovich, L. M.; Gavney, J. A.; Powell, D. R. *J. Am. Chem. Soc.* **1992**, *114*, 5535−5543.
(53) Casey, C. P.; Paulsen, E. L.; Beuttenmueller, E. W.; Proft, B. R.; Petrovich, L. M.; Matter, B. A.; Powell, D. R. *J. Am. Chem. Soc.* **1997**, *119*, 11817−11825.
(54) Casey, C. P.; Paulsen, E. L.; Beuttenmueller, E. W.; Proft, B. R.; Matter, B. A.; Powell, D. R. *J. Am. Chem. Soc.* **1998**, *121*, 63−70.
(55) Malatesta, L.; Angoletta, M.; Conti, F. *J. Organomet. Chem.* **1971**, *33*, C43−C44.
(56) Whyman, R. *J. Organomet. Chem.* **1971**, *29*, C36−C38.
(57) Drakesmith, A. J.; Whyman, R. *J. Chem. Soc., Dalton Trans.* **1973**, 362−367.
(58) Yagupsky, G.; Wilkinson, G. *J. Chem. Soc. A* **1969**, 725−733.
(59) Ciechanowicz, M.; Skapski, A. C.; Troughton, P. G. H. *Acta Crystallogr, Sect. B* **1976**, *32*, 1673−1680.
(60) Bath, S. S.; Vaska, L. *J. Am. Chem. Soc.* **1963**, *85*, 3500−3501.
(61) Vaska, L. *J. Am. Chem. Soc.* **1966**, *88*, 4100−4101.
(62) Whyman, R. *J. Chem. Soc. D: Chem. Commun.* **1969**, 1381−1382.
(63) Whyman, R. *J. Chem. Soc., Dalton Trans.* **1972**, 2294−2296.
(64) Meakin, P.; Muetterties, E. L.; Jesson, J. P. *J. Am. Chem. Soc.* **1972**, *94*, 5271−5285.
(65) Garland, M.; Pino, P. *Organometallics* **1991**, *10*, 1693−1704.
(66) Moasser, B.; Gladfelter, W. L.; Roe, D. C. *Organometallics* **1995**, *14*, 3832−3838.
(67) Güven, S.; Nieuwenhuizen, M. M. L.; Hamers, B.; Franke, R.; Priske, M.; Becker, M.; Vogt, D. *ChemCatChem.* **2014**, *6*, 603−610.
(68) (a) Van Rooy, A.; de Bruijn, J. N. H.; Roobeek, K. F.; Kamer, P. C. J.; Van Leeuwen, P. W. N. M. *J. Organomet. Chem.* **1996**, *507*, 69−73. (b) Doyle, M. P.; Shanklin, M. S.; Zlokazov, M. V. *Synlett* **1994**, *8*, 615−616.
(69) Zuidema, E.; Escorihuela, L.; Eichelsheim, T.; Carbó, J. J.; Bo, C.; Kamer, P. C. J.; van Leeuwen, P. W. N. M. *Chem.—Eur. J.* **2008**, *14*, 1843−1853.
(70) Malatesta, L.; Caglio, G.; Angoletta, M. *J. Chem. Soc.* **1965**, 6974−6983.
(71) Brown, C. K.; Mowat, W.; Yagupsky, G.; Wilkinson, G. *J. Chem. Soc. A* **1971**, 850−859.
(72) Hasnip, S. K.; Colebrooke, S. A.; Sleigh, C. J.; Duckett, S. B.; Taylor, D. R.; Barlow, G. K.; Taylor, M. J. *J. Chem. Soc., Dalton Trans.* **2002**, 743−751.
(73) Whyman, R. *J. Organomet. Chem.* **1975**, *94*, 303−309.
(74) Fisher, B. J.; Eisenberg, R. *Organometallics* **1983**, *2*, 764−767.
(75) Jáuregui-Haza, U. J.; Pardillo-Fontdevila, E. J.; Wilhelm, A. M.; Delmas, H. *Lat. Am. Appl. Res.* **2004**, *34*, 71−74.
(76) Brunner, E. *J. Chem. Eng. Data* **1985**, *30*, 269−273.
(77) Bittrich, H.-J.; Haberland, D.; Just, G. *Leitfaden der chemischen Kinetik, Deutscher Verlag der Wissenschaften*, 2nd edition; Auflage: Berlin, 1986; pp 46−54.
(78) Brown, J. M.; Kent, A. G. *J. Chem. Soc. Perkin Trans. II* **1987**, 1597−1607.
(79) Selent, D.; Baumann, W.; Börner, A. (to Leibniz-Institut für Katalyse e.V.). Gas introduction and circulation apparatus for monitoring reactions in the liquid phase under participation of gaseous reactants under normal and high pressure by means of nuclear resonance spectroscopy (pressure NMR spectroscopy) under stationary conditions. German Patent No.DE 10333143. July 17, 2003. *Chem. Abstr.* **2005**, *142*, 263666.

(80) *TURBOMOLE*, version 6.3.1 2011, a development of University of Karlsruhe and Forschungszentrum Karlsruhe GmbH, 1989−2007; TURBOMOLE GmbH: Karlsruhe, Germany, 2007. Available from http://www.turbomole.com.
(81) (a) Becke, A. D. *Phys. Rev. A* **1988**, *38*, 3098−3100. (b) Perdew, J. P. *Phys. Rev. B* **1986**, *33*, 8822−8824. (c) Perdew, J. P. *Phys. Rev. B* **1986**, *34*, 7406.
(82) Eichkorn, K.; Weigend, F.; Treutler, O.; Ahlrichs, R. *Theor. Chem. Acc.* **1997**, *97*, 119−124.